

A New High-order Time-kernel BIEM for the Burgers Equation

N. Mai-Duy^{1,2}, T. Tran-Cong² and R.I. Tanner³

Abstract: This paper presents a new high-order time-kernel boundary-integral-equation method (BIEM) for numerically solving transient problems governed by the Burgers equation. Instead of using high-order Lagrange polynomials such as quadratic and quartic interpolation functions, the proposed method employs integrated radial-basis-function networks (IRBFNs) to represent the unknown functions in boundary and volume integrals. Numerical implementations of ordinary and double integrals involving time in the presence of IRBFNs are discussed in detail. The proposed method is verified through the solution of diffusion and convection-diffusion problems. A comparison of the present results and those obtained by low-order BIEMs and other methods is also given.

keyword: Burgers equation, Radial-basis-function networks, Transient problems, Time-dependent fundamental solutions, Boundary-integral-equation methods.

1 Introduction

Parabolic differential equations have been employed in a variety of engineering problems. Solutions to these equations can be found by means of numerical discretization methods such as BIEMs, finite-difference (FDMs), finite-element (FEMs) and finite-volume (FVMs) methods. For BIEMs (e.g. [Banerjee and Butterfield (1981); Brebbia, Telles and Wrobel (1984)]), there are several approaches proposed to deal with a time-derivative term. Based on the criterion of fundamental solutions used, they can be classified into two groups. The first group employs time-dependent fundamental solutions, i.e. time derivatives enter the integral representation through the kernel functions, which allows the process of discretization in time and space to be conducted in a similar fashion. The

second group employs stationary fundamental solutions. Some additional treatments for time derivatives are thus required; they generally fall into one of two categories: Laplace transforms and finite-difference schemes.

In the context of time-kernel BIEMs, there are relatively few papers on using high-order interpolation schemes to approximate the unknown functions with respect to time. The case of using quadratic functional variation was reported in [Brebbia, Telles and Wrobel (1984)]. Recently, Grigoriev and Dargush (2002) employed quartic interpolation functions, and their obtained results indicated a significant improvement in accuracy, convergence rate and error distribution.

Radial-basis-function networks have found a wide range of applications in the field of numerical analysis. These networks exhibit good approximation properties. For example, it has been proved that RBFNs are capable of representing any continuous function to a desired level of accuracy by increasing the number of hidden neurons (universal approximation) [Park and Sandberg (1991)]. Madych and Nelson (1990) showed that the multiquadric (MQ) interpolation scheme converges exponentially with respect to the number of data points used. It was found that IRBFNs have higher approximation power than differentiated RBFNs [Mai-Duy and Tran-Cong (2003a)]. There have been widespread applications of RBFNs for the solution of differential equations (e.g. [Mai-Cao and Tran-Cong (2005); Sarler (2005); Shu, Ding and Yeo (2005); La Rocca, Power, La Rocca and Morale (2005)]).

In the present work, MQ-IRBFNs are introduced into the time-kernel BIEM to represent the functional variations for the solution of transient problems governed by the Burgers equation. As with the case of steady problems (stationary fundamental solutions) [Mai-Duy and Tran-Cong (2003b); Mai-Duy and Tanner (2005)], numerical results obtained show that the IRBFN-BIEM attains a significant improvement in accuracy and convergence speed over low-order time-kernel BIEMs.

The remainder of the paper is organized as follows. In Section 2, the governing equations and fundamental solu-

¹ Corresponding author: Telephone +61 7 4631 1324, Fax +61 7 4631 2526, E-mail maiduy@usq.edu.au

² Faculty of Engineering and Surveying, The University of Southern Queensland, QLD 4350, Australia

³ School of Aerospace, Mechanical and Mechatronic Engineering, The University of Sydney, NSW 2006, Australia

tions are outlined. In Section 3, a brief review of IRBFNs is given. The proposed method is then presented in Section 4, followed by several numerical examples in Section 5 to demonstrate the validity and attractiveness of the present implementation. Section 6 gives some concluding remarks.

2 Governing equations

The equation under discussion here is of the form

$$\mu \left(\frac{\partial u}{\partial t} + u \frac{\partial u}{\partial x} \right) = \frac{\partial^2 u}{\partial x^2} \quad (1)$$

where t is the temporal coordinate $0 \leq t \leq t_f$, x the spatial coordinate $a \leq x \leq b$, u the dependent variable, and μ a given parameter, subject to the initial condition

$$u(x, 0) = u_0(x) \quad (2)$$

and a set of Dirichlet and Neumann boundary conditions prescribed at $x = a$ and $x = b$.

By treating the convective term $u\partial u/\partial x$ as a source term, equation (1) can be recast into the following integral equation

$$\begin{aligned} u(\xi, t_f) + \int_0^{t_f} [u(x, t)q^*(\xi, x, t_f, t)]_a^b dt \\ = \int_0^{t_f} \left[\frac{\partial u(x, t)}{\partial x} u^*(\xi, x, t_f, t) \right]_a^b dt \\ + \int_a^b \mu u_0(x) u^*(\xi, x, t_f, 0) dx \\ - \int_a^b \int_0^{t_f} \mu u(x, t) \frac{\partial u(x, t)}{\partial x} u^*(\xi, x, t_f, t) dt dx \end{aligned} \quad (3)$$

where ξ is the source point $a \leq \xi \leq b$, x the field point, u^* and q^* the time-dependent fundamental solutions defined as

$$u^* = \frac{1}{2\sqrt{\pi\mu(t_f-t)}} \exp \left[\frac{-\mu(x-\xi)^2}{4(t_f-t)} \right], \quad \text{for } t < t_f \quad (4)$$

$$u^* = 0, \quad \text{for } t > t_f \quad (5)$$

$$q^* = \frac{\partial u^*}{\partial x} = \frac{-\sqrt{\mu}(x-\xi)}{4\sqrt{\pi}(t_f-t)^{3/2}} \exp \left[\frac{-\mu(x-\xi)^2}{4(t_f-t)} \right] \quad (6)$$

These fundamental solutions depend not only on the variable x and the source point ξ but also on the variable t and

the time t_f . It can be seen that the singularity occurs for u^* when $x \rightarrow \xi$ and $t \rightarrow t_f$. More details can be found in [Banerjee and Butterfield (1981); Brebbia, Telles and Wrobel (1984)].

3 Integrated Radial-Basis-Function Networks

Consider a function $f(\eta)$. The independent variable η can be taken to be time t or space x . In the IRBFN scheme [Mai-Duy and Tran-Cong (2003a)], the second-order derivative $\partial^2 f/\partial \eta^2$ is decomposed into RBFs. The RBF network obtained is then integrated to yield expressions for the first-order derivative and its original function

$$\frac{d^2 f(\eta)}{d\eta^2} = \sum_{i=1}^m w^{(i)} g^{(i)}(\eta) \quad (7)$$

$$\frac{df(\eta)}{d\eta} = \int \sum_{i=1}^m w^{(i)} g^{(i)}(\eta) d\eta + C_1 = \sum_{i=1}^{m+1} w^{(i)} H_{[1]}^{(i)}(\eta) \quad (8)$$

$$f(\eta) = \int \sum_{i=1}^m w^{(i)} H_{[1]}^{(i)} d\eta + C_1 \eta + C_2 = \sum_{i=1}^{m+2} w^{(i)} H_{[0]}^{(i)}(\eta) \quad (9)$$

where superscript (i) is used to denote components associated with the i th neuron, m is the number of neurons, $\{g^{(i)}\}_{i=1}^m$ the set of RBFs, $\{w^{(i)}\}_{i=1}^m$ the set of network weights to be found, and $\{H_{[1]}^{(i)}\}_{i=1}^m$ new basis functions obtained from integrating $\{g^{(i)}\}_{i=1}^m$. For convenience of presentation, integration constants which are unknowns here and their associated known basis functions (polynomials) on the right-hand side (RHS) of (8)-(9) are also denoted by the notations $w^{(i)}$ and $H_{[1]}^{(i)}$, respectively but with $i > m$.

Among RBFs, multiquadrics (MQs) are the most widely used since several experiments have shown that, in general, they tend to result in the most accurate approximation. Madych and Nelson (1990) showed that the MQ interpolation scheme exhibits an exponential convergence. In the present work, the MQ function is utilized and hence the basis functions $g^{(i)}$ and $H_{[1]}^{(i)}$ ($i = 1, 2, \dots, m$) take the forms as

$$g^{(i)}(\eta) = \sqrt{(\eta - c^{(i)})^2 + a^{(i)2}} \quad (10)$$

$$H_{[1]}^{(i)}(\eta) = \frac{(\eta - c^{(i)})}{2} A + \frac{a^{(i)2}}{2} B \quad (11)$$

$$H_{[0]}^{(i)}(\eta) = \left(\frac{-a^{(i)2}}{3} + \frac{(\eta - c^{(i)})^2}{6} \right) A + \frac{a^{(i)2}(\eta - c^{(i)})}{2} B \quad \text{or} \quad \mathbf{w} = \mathbf{H}_{[0]}^{-1} \mathbf{f} \quad (12)$$

where $\{c^{(i)}\}_{i=1}^m$ is the set of RBF centres, $\{a^{(i)}\}_{i=1}^m$ the set of RBF widths, $A = \sqrt{(\eta - c^{(i)})^2 + a^{(i)2}}$ and $B = \ln \left((\eta - c^{(i)}) + \sqrt{(\eta - c^{(i)})^2 + a^{(i)2}} \right)$. The set of centres is chosen to be the same as the set of collocation points, i.e. $\{c^{(i)}\}_{i=1}^m \equiv \{x^{(i)}\}_{i=1}^n$ with $m = n$, and the width $a^{(i)}$ is computed using the following relation

$$a^{(i)} = \beta d^{(i)} \quad (13)$$

where β is a positive scalar and $d^{(i)}$ is the minimum distance from the i th centre to its neighbours.

It is more convenient to work in physical space than in network-weight space. The evaluation of (9) at the set of collocation points $\{\eta^{(i)}\}_{i=1}^n$ results in

$$\begin{pmatrix} f(\eta^{(1)}) \\ f(\eta^{(2)}) \\ \vdots \\ f(\eta^{(n)}) \end{pmatrix} = \begin{bmatrix} H_{[0]}^{(1)}(\eta^{(1)}) & \cdots & H_{[0]}^{(m)}(\eta^{(1)}) & \eta^{(1)} & 1 \\ H_{[0]}^{(1)}(\eta^{(2)}) & \cdots & H_{[0]}^{(m)}(\eta^{(2)}) & \eta^{(2)} & 1 \\ \cdots & & & & \\ H_{[0]}^{(1)}(\eta^{(n)}) & \cdots & H_{[0]}^{(m)}(\eta^{(n)}) & \eta^{(n)} & 1 \end{bmatrix} \begin{pmatrix} w^{(1)} \\ w^{(2)} \\ \vdots \\ w^{(m+2)} \end{pmatrix} \frac{df(\eta)}{d\eta} = \begin{bmatrix} H_{[1]}^{(1)}(\eta) & \cdots & H_{[1]}^{(m)}(\eta) & 1 & 0 \\ f^{(1)} f^{(2)} & \cdots & f^{(n)} \end{bmatrix} \mathbf{H}_{[0]}^{-1} \quad (14)$$

4 The proposed IRBFN-BIEM

The obtained system (14) for the unknown vector of network weights can be solved using the SVD technique

$$\begin{pmatrix} w^{(1)} \\ w^{(2)} \\ \vdots \\ w^{(m+2)} \end{pmatrix} = \begin{bmatrix} H_{[0]}^{(1)}(\eta^{(1)}) & \cdots & H_{[0]}^{(m)}(\eta^{(1)}) & \eta^{(1)} & 1 \\ H_{[0]}^{(1)}(\eta^{(2)}) & \cdots & H_{[0]}^{(m)}(\eta^{(2)}) & \eta^{(2)} & 1 \\ \cdots & & & & \\ H_{[0]}^{(1)}(\eta^{(n)}) & \cdots & H_{[0]}^{(m)}(\eta^{(n)}) & \eta^{(n)} & 1 \end{bmatrix}^{-1} \begin{pmatrix} f(\eta^{(1)}) \\ f(\eta^{(2)}) \\ \vdots \\ f(\eta^{(n)}) \end{pmatrix} \quad (15)$$

where $\mathbf{H}_{[0]}^{-1}$ is the Moore-Penrose pseudoinverse, and \mathbf{w} , $\mathbf{H}_{[0]}$ and \mathbf{f} are matrices of dimension $(m+2) \times 1$, $n \times (m+2)$ and $n \times 1$, respectively. From (15)-(16), it can be seen that the network weights $\{w^{(i)}\}_{i=1}^{m+2}$ are expressed in terms of the function values $\{f^{(i)}\}_{i=1}^n$. By substituting (16) into (7)-(9), the function f and its derivatives at an arbitrary point η can be computed by

$$f(\eta) = \begin{bmatrix} H_{[0]}^{(1)}(\eta) & \cdots & H_{[0]}^{(m)}(\eta) & \eta & 1 \end{bmatrix} \mathbf{H}_{[0]}^{-1} \begin{bmatrix} f^{(1)} f^{(2)} & \cdots & f^{(n)} \end{bmatrix}^T \quad (17)$$

$$\frac{df(\eta)}{d\eta} = \begin{bmatrix} H_{[1]}^{(1)}(\eta) & \cdots & H_{[1]}^{(m)}(\eta) & 1 & 0 \end{bmatrix} \mathbf{H}_{[0]}^{-1} \begin{bmatrix} f^{(1)} f^{(2)} & \cdots & f^{(n)} \end{bmatrix}^T \quad (18)$$

$$\frac{d^2f(\eta)}{d\eta^2} = \begin{bmatrix} g^{(1)}(\eta) & \cdots & g^{(m)}(\eta) & 0 & 0 \end{bmatrix} \mathbf{H}_{[0]}^{-1} \begin{bmatrix} f^{(1)} f^{(2)} & \cdots & f^{(n)} \end{bmatrix}^T \quad (19)$$

The temporal domain of interest $[0, t_f]$ is represented by a set of n_t uniformly/non-uniformly distributed points: $\{t^{(1)} = 0, t^{(2)}, \dots, t^{(n_t)} = t_f\}$. There are $2(n_t - 1)$ nodal unknowns (u or $\partial u / \partial x$) on the boundaries so that one needs to write $2(n_t - 1)$ algebraic equations. This can be achieved by writing the BIE (3) at $x = a$ and $x = b$ for different time levels $\{t^{(2)}, t^{(3)}, \dots, t^{(n_t)}\}$:

$$\begin{aligned} u(a, t^{(i)}) + \int_0^{t^{(i)}} \left[u(x, t) q^*(a, x, t^{(i)}, t) \right]_a^b dt \\ = \int_0^{t^{(i)}} \left[\frac{\partial u(x, t)}{\partial x} u^*(a, x, t^{(i)}, t) \right]_a^b dt \\ + \int_a^b \mu u_0(x) u^*(a, x, t^{(i)}, 0) dx \\ - \int_a^b \int_0^{t^{(i)}} \mu u(x, t) \frac{\partial u(x, t)}{\partial x} u^*(a, x, t^{(i)}, t) dt dx \end{aligned} \quad (20)$$

$$\begin{aligned}
 u(b, t^{(i)}) + \int_0^{t^{(i)}} \left[u(x, t) q^*(b, x, t^{(i)}, t) \right]_a^b dt \\
 = \int_0^{t^{(i)}} \left[\frac{\partial u(x, t)}{\partial x} u^*(b, x, t^{(i)}, t) \right]_a^b dt \\
 + \int_a^b \mu u_0(x) u^*(b, x, t^{(i)}, 0) dx \\
 - \int_a^b \int_0^{t^{(i)}} \mu u(x, t) \frac{\partial u(x, t)}{\partial x} u^*(b, x, t^{(i)}, t) dt dx \quad (21)
 \end{aligned}$$

where $i = \{2, 3, \dots, n_t\}$. It can be seen that BIEs (20)-(21) involve ordinary and double integrals. Here, the unknown functions in these integrals are approximated by using IRBFNs. The objective now is to express the integrals in terms of nodal variable values. For brevity, consider a generic case

$$I = \int_a^b \int_0^{t_f} f(x, t) u^*(x, t) dt dx \quad (22)$$

where $f(x, t)$ is an unknown function represented by an IRBFN (17). This integral can be computed in a sequential manner (iterated integrals) as follows

$$I = \int_a^b \left\{ \int_0^{t_f} f(x, t) u^*(x, t) dt \right\} dx \quad (23)$$

4.1 Integration with respect to time

The bracketed integration in (23) is performed with respect to t , regarding x as constant (\bar{x})

$$\int_0^{t_f} f(\bar{x}, t) u^*(\bar{x}, t) dt = \sum_{i=1}^{n_t-1} \int_{t^{(i)}}^{t^{(i+1)}} f(\bar{x}, t) u^*(\bar{x}, t) dt \quad (24)$$

The integrals on the RHS of (24) can be computed using Gaussian quadrature. At the base points, the values of the kernel function $u^*(\bar{x}, t)$ are evaluated explicitly, while the values of the function $f(\bar{x}, t)$ are written in terms of its nodal values

$$\left\{ f(\bar{x}, t^{(1)}), f(\bar{x}, t^{(2)}), \dots, f(\bar{x}, t^{(n_t)}) \right\}$$

using the IRBFN scheme (17). Expression (24) can thus be rewritten in a compact form

$$\int_0^{t_f} f(\bar{x}, t) u^*(\bar{x}, t) dt = \sum_{i=1}^{n_t} \psi(\bar{x}, t^{(i)}) f(\bar{x}, t^{(i)}) \quad (25)$$

where $\psi(\bar{x}, t^{(i)})$ is the known function.

Applying (25) to $\bar{x} = a$ and $\bar{x} = b$, the discrete forms of the first integral on the RHS of (3) are obtained. It is noted that when $i = (n_t - 1)$ the corresponding integral becomes weakly singular due to the presence of the term $1/\sqrt{t_f - t}$. One can use a coordinate transformation ($T = \sqrt{t_f - t}$, T : a new variable) to cancel out this singularity. Substitution of (25) into (23) yields

$$I = \int_a^b \sum_{i=1}^{n_t} \psi(x, t^{(i)}) f(x, t^{(i)}) dx \quad (26)$$

4.2 Integration with respect to space

The spatial domain $[a, b]$ is discretized by a set of n_x points of uniform/nonuniform distribution: $\{x^{(1)} = a, x^{(2)}, \dots, x^{(n_x)} = b\}$

$$I = \sum_{j=1}^{n_x-1} \int_{x^{(j)}}^{x^{(j+1)}} \sum_{i=1}^{n_t} \psi(x, t^{(i)}) f(x, t^{(i)}) dx \quad (27)$$

Gaussian quadrature can be utilized to compute integrals in (27). At the integration points, the values of the function $\psi(x, t^{(i)})$ are obtained explicitly, while the values of the function $f(x, t^{(i)})$ are expressed in terms of its nodal values:

$$\{f(x^{(1)}, t^{(i)}), f(x^{(2)}, t^{(i)}), \dots, f(x^{(n_x)}, t^{(i)})\}$$

by means of IRBFNs (17).

Finally, one can write the integral I in terms of nodal values of the unknown function f over the whole temporal-spatial domain

$$I = \sum_{j=1}^{n_x} \sum_{i=1}^{n_t} \Phi(x^{(j)}, t^{(i)}) f(x^{(j)}, t^{(i)}) \quad (28)$$

where $\Phi(x, t)$ is the known function.

5 Numerical results

A number of examples are included in this section to demonstrate the attractiveness of the present implementation. In the following test cases, the width of the i th neuron ($a^{(i)}$) is simply chosen to be the minimum distance from the i th centre to neighbouring centres. The accuracy of a numerical solution produced by an approximation scheme can be measured via a root-mean-square residual

$$RMS = \sqrt{\frac{\sum_{j=1}^{n_x} \sum_{i=1}^{n_t} [u_e(x^{(j)}, t^{(i)}) - u(x^{(j)}, t^{(i)})]^2}{n_t n_x}} \quad (29)$$

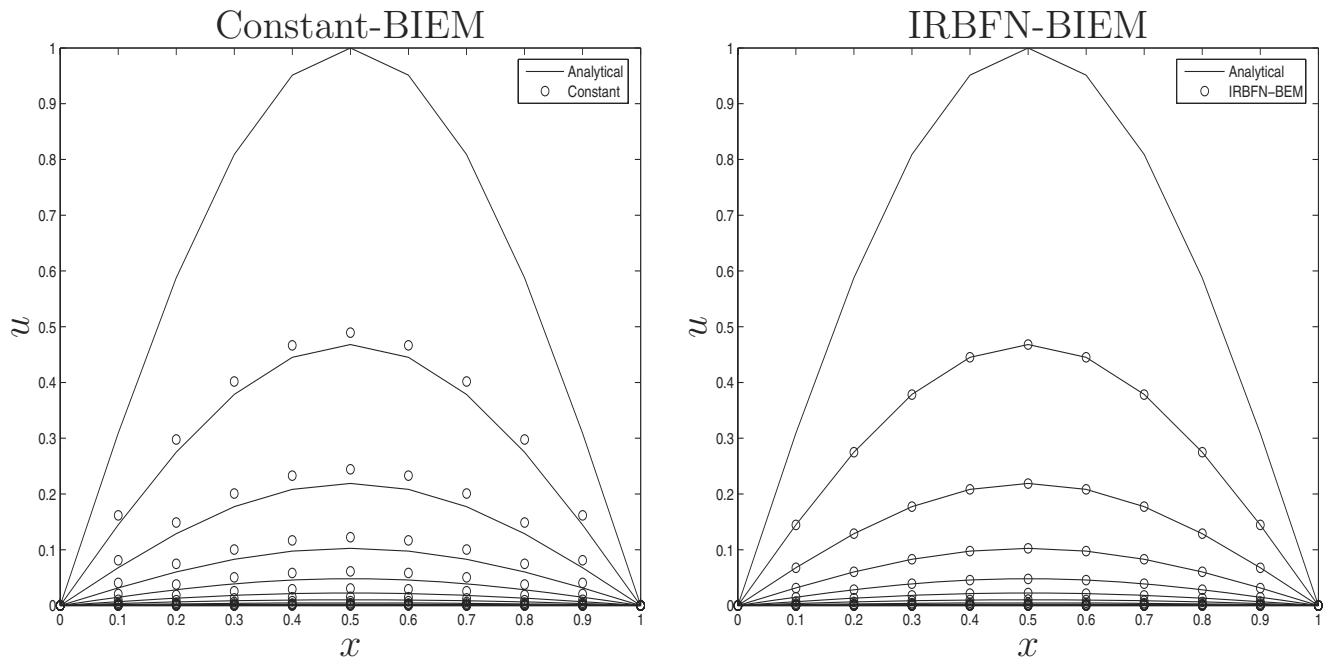


Figure 1 : Example 1, diffusion problem, $0 \leq t, x \leq 1$, $n_x = 11$, $n_t = 14$: the evolution of the solution u by constant- and IRBFN-BIEMs.

where n_t and n_x are the numbers of points used for the temporal and spatial discretizations, respectively, and u and u_e are the calculated and exact solutions, respectively.

5.1 Example 1, diffusion problem

The proposed method is first tested through the solution of a simplified form of (1). Consider a diffusion problem governed by

$$\frac{\partial u}{\partial t} = \frac{\partial^2 u}{\partial x^2} \quad (30)$$

in a planar domain ($0 \leq x, t \leq 1$) with Dirichlet boundary conditions

$$u(0, t) = 0 \quad (31)$$

$$u(1, t) = 0 \quad (32)$$

and the initial solution

$$u(x, 0) = \sin(\pi x) \quad (33)$$

The exact solution of this problem is given by Carslaw and Jaeger (1959)

$$u_e = \exp(-\pi^2 t) \sin(\pi x) \quad (34)$$

Since there are no source terms here, the double integral on the RHS of (3) is discarded.

To provide the basis for the assessment of the presently proposed IRBFN-BIEM, low-order BIEMs are also considered here. The temporal domain is divided into a number of intervals. There are two principal time-marching schemes available in the BIEM literature, namely the time-recurring initial condition and convolution approaches. The former treats each time interval as a new problem, while the latter always starts the time integration process at $t = 0$. Since information from all previous time steps are used to calculate the current integrals, the convolution approach is seen to be more accurate than the time-recurring initial condition approach [Ramachandran (1994)]. Complete computational details can be found in [Banerjee and Butterfield (1981); Brebbia, Telles and Wrobel (1984)]. Results presented here for comparison purposes are obtained using constant elements and the convolution approach. In the proposed IRBFN-BIE approach, global IRBFN interpolation schemes are employed to represent the variation with time for the variable $\partial u / \partial x$. An incremental time between two successive points along the time axis is also referred to as time step. It is instructive to note that the present boundary solutions over the temporal domain of

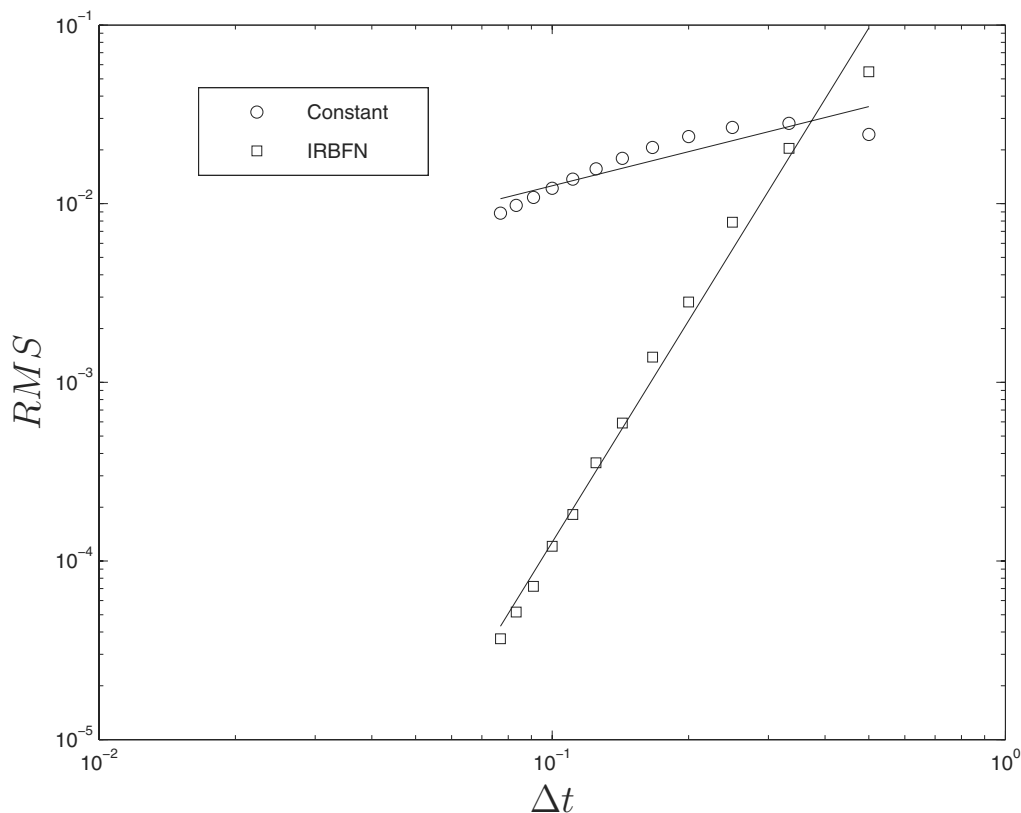


Figure 2 : Example 1, diffusion problem, $0 \leq t, x \leq 1$, $n_x = 11$, $n_t = \{3, 4, \dots, 14\}$: accuracy and convergence rate obtained by constant- and IRBFN-BIEMs.

interest are obtained at once rather than step by step as in the case of low-order BIEMs.

For both approaches, i.e. constant- and IRBFN-BIEMs, volume integrals generated by the initial solution are simply computed by standard Gaussian quadrature. The spatial domain is discretized using 11 uniformly distributed points.

Figure 1 displays the evolution of the solution u from $t = 0$ to $t = 1$ using $n_t = 14$ by the constant- and IRBFN-BIEMs. More accurate results are obtained with the present method. To study the convergence behaviour with time refinement, a number of time steps, $n_t = \{3, 4, \dots, 14\}$, are employed. The IRBFN-BIEM is far superior to the constant-BIEM in terms of convergence and accuracy as shown in Figure 2. The convergence rates obtained are of $O(\Delta t^{0.63})$ and $O(\Delta t^{4.12})$ for the constant- and IRBFN-BIEMs, respectively.

In the case of non-smooth time-dependent boundary conditions, it is necessary to decompose the temporal domain into several subdomains, over each of which the

boundary data are continuous. It thus allows the use of the IRBFN-BIEM over each subdomain. Solutions will be then obtained step by step as in the case of finite differences.

The proposed method yields a much higher level of accuracy than conventional techniques. However, the construction of the IRBFN approximations requires more computational effort than that of approximations based on low-order polynomials.

5.2 Example 2, diffusion problem

This problem is the same as the previous one, except the initial solution is replaced by

$$u(x, 0) = \begin{cases} 2x & \text{if } 0 \leq x \leq 0.5 \\ 2(1-x) & \text{if } 0.5 \leq x \leq 1.0 \end{cases} \quad (35)$$

The analytical solution given by Carslaw and Jaeger (1959) is

$$u_e(x, t) = \frac{8}{\pi^2} \sum_{k=1}^{\infty} \frac{1}{k^2} \sin \frac{k\pi}{2} \sin k\pi x \exp(-(k\pi)^2 t) \quad (36)$$

Table 1 : Example 2, diffusion problem, $0 \leq x \leq 1$, $0 \leq t \leq 0.25$: temperature at the centre of the slab obtained by the present method and various finite difference methods (FDMs).

$u(\text{error } \%)$					
t	FDM-CN	FDM-PI	FDM-WT	IRBFN-BIEM	Exact
0.025	0.5637(12.35)	0.6888(7.09)	0.6807(5.84)	0.6432(0.00)	0.6432
0.05	0.5440(9.69)	0.5330(7.47)	0.5286(6.58)	0.4959(0.01)	0.4959
0.075	0.3493(9.68)	0.4226(9.27)	0.4188(8.29)	0.3867(0.01)	0.3868
0.1	0.3313(9.66)	0.3376(11.76)	0.3341(10.58)	0.3021(0.01)	0.3021
0.125	0.2117(10.31)	0.2705(14.58)	0.2671(13.14)	0.2360(0.01)	0.2360
0.15	0.2038(10.50)	0.2169(17.60)	0.2137(15.86)	0.1844(0.01)	0.1844
0.175	0.1270(11.84)	0.1740(20.74)	0.1710(18.67)	0.1441(0.01)	0.1441
0.2	0.1262(12.10)	0.1396(20.99)	0.1369(21.57)	0.1126(0.01)	0.1126
0.225	0.0756(14.12)	0.1120(27.33)	0.1096(24.54)	0.0880(0.01)	0.0880
0.25	0.0787(14.47)	0.0899(30.76)	0.0877(27.58)	0.0687(0.01)	0.0687

Table 2 : Example 3, Burgers equation, $Re = 1$, $t_f = 0.22$, $\Delta x = 0.1$, $\Delta t = 0.02$: Solution profiles at some time levels. Results by the generalized BIEM (GBIEM) using $\Delta x = 0.05$ and $\Delta t = 0.02$ are also included for comparison.

$u(\text{error } \%)$						
x	$t = 0.1$			$t = 0.22$		
	GBIEM	Present	Exact	GBIEM	Present	Exact
0.1	0.11718(6.97)	0.10956(0.02)	0.10954	0.03972(15.00)	0.03455(0.03)	0.03454
0.2	0.22436(6.95)	0.20979(0.00)	0.20979	0.07578(15.06)	0.06586(0.00)	0.06586
0.3	0.31202(6.89)	0.29190(0.00)	0.29190	0.10478(15.13)	0.09101(0.00)	0.09100
0.4	0.37168(6.83)	0.34793(0.00)	0.34792	0.12390(15.25)	0.10751(0.00)	0.10751
0.5	0.39668(6.75)	0.37158(0.00)	0.37158	0.13112(15.35)	0.11367(0.00)	0.11367
0.6	0.38303(6.68)	0.35905(0.00)	0.35905	0.12552(15.47)	0.10870(0.00)	0.10870
0.7	0.33040(6.61)	0.30991(0.00)	0.30991	0.10741(15.57)	0.09293(0.01)	0.09294
0.8	0.24277(6.56)	0.22782(0.00)	0.22782	0.07841(15.67)	0.06779(0.00)	0.06779
0.9	0.12856(6.52)	0.12071(0.02)	0.12069	0.04135(15.73)	0.03574(0.02)	0.03573

Haberland and Lahrman (1988) used FDMs to solve this problem, where a comparative investigation on recurrence formulae such as the Euler, Crank-Nicolson (CN), Pure Implicit (PI) and Weighted time step (WI) schemes was conducted. Their results with $\Delta t = 0.025$ and $\Delta x = 0.05$ are included here for comparison purposes (Table 1). Using the same time step ($\Delta t = 0.025$) and a coarser spatial discretization ($\Delta x = 0.1$), the present method yields superior accuracy. For example, the maximum error is 0.01% for IRBFN-BIEM while they are

14.47%, 30.76% and 27.58% for FDM-CN, FDM-PI and FDM-WI, respectively.

5.3 Example 3, convection-diffusion problem

This example consider a non-linear partial differential equation, the Burgers equation (1). This equation has a structure similar to the Navier-Stokes equation. Although it is nonlinear, the Burgers equation can be solved analytically for many combinations of initial and boundary conditions. It is thus used as a simple model for the

Table 3 : Example 3, Burgers equation, $Re = 10, t_f = 1.5, \Delta x = 0.1, \Delta t = 0.05$: Solution profiles at some time levels. Results by the generalized BIEM (GBIEM) using $\Delta x = 0.025$ and $\Delta t = 0.05$ are also included.

$u(\text{error } \%)$						
x	$t = 0.75$			$t = 1.5$		
	GBIEM	Present	Exact	GBIEM	Present	Exact
0.1	0.08649(3.67)	0.08342(0.01)	0.08343	0.04521(3.34)	0.04375(0.01)	0.04374
0.2	0.17146(3.59)	0.16551(0.00)	0.16552	0.08868(3.42)	0.08575(0.00)	0.08575
0.3	0.25289(3.44)	0.24447(0.00)	0.24448	0.12830(3.52)	0.12394(0.00)	0.12394
0.4	0.32767(3.24)	0.31738(0.00)	0.31738	0.16127(3.67)	0.15557(0.00)	0.15556
0.5	0.39026(2.99)	0.37892(0.00)	0.37892	0.18378(3.88)	0.17691(0.00)	0.17691
0.6	0.43060(2.71)	0.41923(0.00)	0.41922	0.19089(4.16)	0.18327(0.00)	0.18327
0.7	0.43120(2.44)	0.42095(0.01)	0.42093	0.17721(4.47)	0.16963(0.01)	0.16962
0.8	0.36690(2.21)	0.35904(0.02)	0.35896	0.13888(4.79)	0.13254(0.01)	0.13253
0.9	0.21751(2.06)	0.21319(0.03)	0.21312	0.07691(5.03)	0.07324(0.01)	0.07323

Table 4 : Example 3, Burgers equation, $Re = 100, t_f = 3.0, \Delta x = 0.02, \Delta t = 0.1, \text{relax}=0.1$: Solution profiles at some time levels. Results by the generalized BIEM (GBIEM) using $\Delta x = 0.01$ and $\Delta t = 0.01$ are also included.

$u(\text{error } \%)$						
x	$t = 1.2$			$t = 3.0$		
	GBIEM	Present	Exact	GBIEM	Present	Exact
0.2	0.13173(0.62)	0.13092(0.00)	0.13092	0.06036(0.44)	0.06010(0.01)	0.06009
0.4	0.26285(0.60)	0.26127(0.01)	0.26128	0.12068(0.43)	0.12015(0.00)	0.12016
0.6	0.39264(0.56)	0.39043(0.00)	0.39044	0.18095(0.43)	0.18018(0.00)	0.18018
0.8	0.52012(0.50)	0.51756(0.01)	0.51753	0.23906(0.18)	0.23861(0.00)	0.23863
0.9	0.57950(0.29)	0.57780(0.00)	0.57781	0.23766(1.63)	0.24158(0.00)	0.24159
0.92	0.58466(0.01)	0.58482(0.02)	0.58472	0.22050(2.48)	0.22616(0.00)	0.22612
0.94	0.57336(0.77)	0.57760(0.03)	0.57779	0.18997(3.51)	0.19696(0.01)	0.19690
0.96	0.51253(2.42)	0.52551(0.05)	0.52524	0.14228(4.58)	0.14915(0.01)	0.14911
0.98	0.33294(5.04)	0.35023(0.11)	0.35060	0.07698(5.41)	0.08140(0.01)	0.08139

understanding of physical flows and the testing of the performance of numerical methods [Fletcher (1984)].

The spatial domain, boundary conditions and initial condition are defined as

$$\begin{aligned}
 a &= 0, \quad b = 1 \\
 u(0, t) &= u(1, t) = 0 \\
 u_0 &= \sin(\pi x)
 \end{aligned}$$

Here, the parameter μ can be regarded as the Reynolds number Re . The analytical solution to this problem was given in the form of an infinite series by Cole (1951)

$$u(x, t) = \frac{4\pi}{\mu l} \frac{\sum_{k=1}^{\infty} \exp(-\frac{k^2 \pi^2 t}{\mu l^2}) k I_k(\frac{l\mu}{2\pi}) \sin(\frac{k\pi x}{l})}{I_0(\frac{l\mu}{2\pi}) + 2 \sum_{k=1}^{\infty} \exp(-\frac{k^2 \pi^2 t}{\mu l^2}) I_k(\frac{l\mu}{2\pi}) \cos(\frac{k\pi x}{l})}$$

(37)

where $l = b - a$ and I_k represents the modified Bessel function of order k . However, it is not practical to obtain the analytical solution for $Re > 10^2$ due to the fact that the magnitude of $I_k(l\mu/2\pi)$ on the RHS of (37) exceeds the limit of the computer precision [Hon and Mao (1998)]. A Picard-type iteration scheme is employed to handle the non-linearity of the system matrix. In the calculation of the convective term, the present work employs the IRBFN scheme to compute the derivative of the function u , which is more straightforward than the case of using the BIE for $\partial u / \partial x$. Results concerning the solution u at some different time levels for $Re = \{1, 10, 100\}$ are given in Tables 2–4, respectively. The corresponding results obtained by the generalized BIEM (GBIEM)

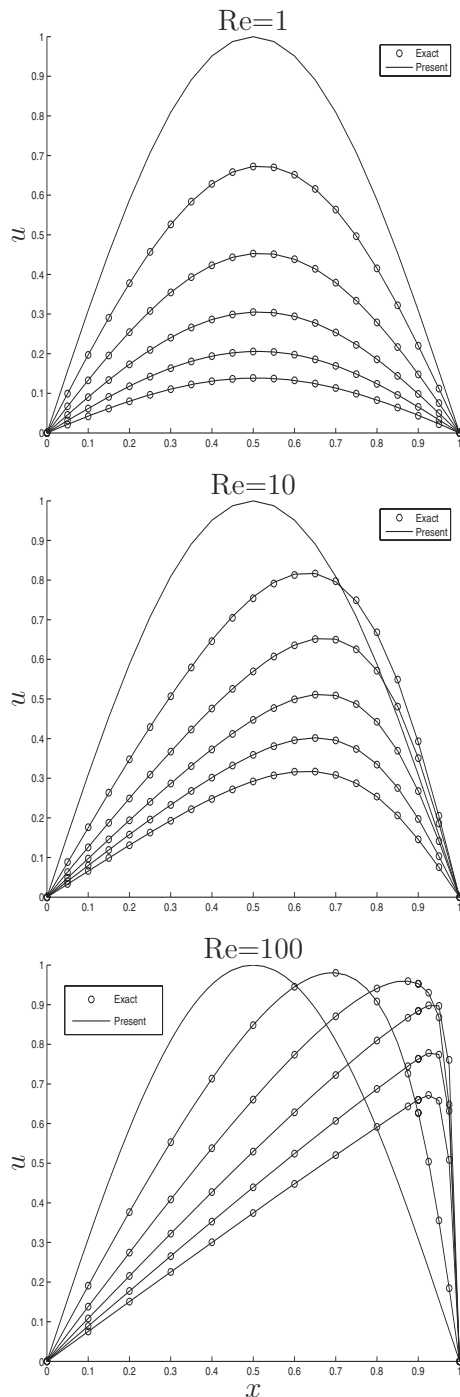


Figure 3 : Example 3, convection-diffusion problem: the evolution of the solution u for several values of the Reynolds number. For $Re = 1$, the parameters used are $t_f = 0.2, n_t = 6$ and $n_x = 21$; for $Re = 10$: $t_f = 1, n_t = 6$ and $n_x = 21$; and for $Re = 100$: $t_f = 1, n_t = 21$ and $n_x = 41$ (time levels displayed: $\{0, 0.2, 0.4, 0.6, 0.8, 1\}$).

[Kakuda and Tosaka (1990)], where the domain is divided into a number of subdomains and the BIE with the time-dependent convective kernel is applied for each subdomain, are also included for comparison. The present results are far superior to those of the GBIEM using linear and constant elements, and in addition, their errors do not accumulate in time. The evolution of the solution u is depicted in Figure 3.

6 Concluding remarks

In this paper, a high-order interpolation scheme, namely integrated RBFNs, is introduced into the time-kernel BIEM to approximate the unknown functions in boundary and volume integrals for the solution of the Burgers equation. All relevant integrals are written in terms of nodal variable values. Solutions over the temporal domain can be obtained at once rather than step by step as in the case of conventional BIEMs. Numerical results show that the method yields a high degree of accuracy and a very fast convergence.

Acknowledgement: This work was supported by the Australian Research Council.

References

Banerjee, P.K.; Butterfield, R. (1981): *Boundary Element Methods in Engineering Science*. McGraw-Hill, London.

Brebbia, C.A.; Telles, J.C.F.; Wrobel, L.C. (1984): *Boundary Element Techniques Theory and Applications in Engineering*. Springer-Verlag, Berlin.

Carslaw, H.S.; Jaeger, J.C. (1959): *Conduction of Heat in Solids*. Clarendon Press, Oxford.

Cole, J.D. (1951): On a quasi-linear parabolic equation occurring in aerodynamics. *Quarterly of Applied Mathematics*, vol. 9(3), pp. 225–236.

Fletcher, C.A.J. (1984): *Computational Galerkin Methods*. Springer-Verlag, New York.

Grigoriev, M.M.; Dargush, G.F. (2002): Higher-order boundary element methods for transient diffusion problems. Part I: bounded flux formulation. *International Journal for Numerical Methods in Engineering* vol. 55, pp. 1–40.

Haberland, C.; Lahrman, A. (1988): A comparative investigation on recurrence formulae in finite difference

methods. *International Journal for Numerical Methods in Engineering*, vol. 25, pp. 593–609.

Hon, Y.C.; Mao, X.Z. (1998): An efficient numerical scheme for Burgers' equation. *Applied Mathematics and Computation*, vol. 95, pp. 37–50.

Kakuda, K.; Tosaka, N. (1990): The generalized boundary element approach to Burgers' equation. *International Journal for Numerical Methods in Engineering*, vol. 29, pp. 245–261.

La Rocca, A.; Power, H.; La Rocca, V.; Morale, M. (2005): A meshless approach based upon radial basis function hermite collocation method for predicting the cooling and the freezing times of foods. *CMC: Computers, Materials & Continua*, vol. 2(4), pp. 239–250.

Madych, W.R.; Nelson, S.A. (1990): Multivariate interpolation and conditionally positive definite functions, II. *Mathematics of Computation*, vol. 54(189), pp. 211–230.

Mai-Cao, L.; Tran-Cong, T. (2005): A meshless IRBFN-based method for transient problems. *CMES: Computer Modeling in Engineering & Sciences*, vol. 7(2), pp. 149–171.

Mai-Duy, N.; Tanner, R.I. (2005): An effective high order interpolation scheme in BIEM for biharmonic boundary value problems. *Engineering Analysis with Boundary Elements*, vol. 29, pp. 210–223.

Mai-Duy, N.; Tran-Cong, T. (2003a): Approximation of function and its derivatives using radial basis function networks. *Applied Mathematical Modelling*, vol. 27, pp. 197–220.

Mai-Duy, N.; Tran-Cong, T. (2003b): RBF interpolation of boundary values in the BIEM for heat transfer problems. *International Journal of Numerical Methods for Heat & Fluid Flow*, vol. 13(5), pp. 611–632.

Park, J.; Sandberg, I.W. (1991): Universal approximation using radial basis function networks. *Neural Computation*, vol. 3, pp. 246–257.

Ramachandran, P.A. (1994): *Boundary Element Methods in Transport Phenomena*. Computational Mechanics Publications, Glasgow.

Sarler, B. (2005): A radial basis function collocation approach in computational fluid dynamics. *CMES: Computer Modeling in Engineering & Sciences*, vol. 7(2), pp. 185–194

Shu, C.; Ding, H.; Yeo, K.S. (2005): Computation of

incompressible navier-stokes equations by local RBF-based differential quadrature method. *CMES: Computer Modeling in Engineering & Sciences*, vol. 7(2), pp. 195–206.